Friction

Research Article

Refreezing of frictional meltwater behind a sliding ski

Michael Hasler[1,2,✉], Werner Jud[1], Joost van Putten[1,2], Werner Nachbauer[1,2]

Cite this article: Hasler M., Jud W., van Putten J., et al. *Friction* 2026, **14**(4): 9441179. https://doi.org/10.26599/FRICT.2025.9441179

ABSTRACT: Low friction on snow has been attributed to the formation of a frictional meltwater layer for many years, yet experimental evidence for this mechanism has remained inconsistent. In a large-scale snow tribometer lab, we measured the snow surface temperature behind a sliding cross-country ski and a flat sliding sample with an infrared camera to study the meltwater film at realistic skiing conditions. At speeds ranging from 5 to 25 m/s and an initial snow temperature of −3.5 °C, surface temperatures increased locally to as high as −0.09 °C. At 15 and 25 m/s, the temperature decay following a ski passage deviated notably from the expected exponential cooling behavior. Instead, the post-passage temperature profile exhibited two distinct phases: an initial slow decline, attributed to latent heat release during the freezing of meltwater, followed by a phase of exponential cooling. This two-phase behavior provides clear evidence for the presence of frictionally generated meltwater. Although the presence of meltwater was most clearly observed after repeated passes over the same track and only at the higher speed, its presence at lower speed or during initial runs cannot be ruled out. The infrared system monitored only the exposed snow surface and may have missed transient meltwater that refroze beneath the ski.

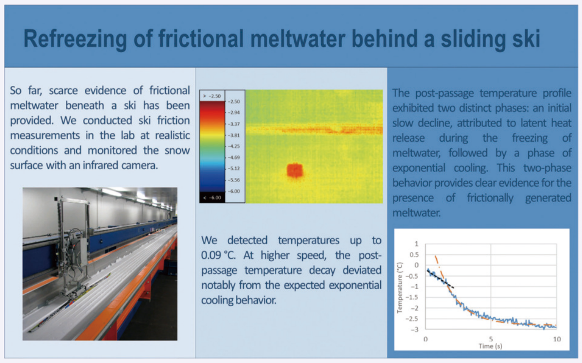

KEYWORDS: ski gliding; snow; tribometer; cross country ski; meltwater; water film; contact pressure

1 Introduction

Lubricated friction has long been recognized as a key mechanism enabling the easy gliding of skis on snow and has been held responsible for this effect since 1939 [1, 2]. However, despite the considerable time that has passed since this hypothesis was first proposed, experimental evidence supporting it remains scarce. For example, Ambach and Mayr [3] used a capacitive sensor to detect a water film up to 20 μm thick. However, this result was strongly challenged [4]. In our own capacitive measurements (unpublished) of up to 10 m/s on fine man-made snow using a flat sample as in the present paper, we could not detect any water film. Other experiments, conducted under unrealistic skiing conditions, failed to detect any trace of meltwater [5, 6].

The long-established theory for characterizing ski-snow friction uses a Stribeck curve to describe friction as a function of the thickness of a water film [2]. Part of the curve has already been falsified when the friction was measured to be very low, even without a detectable water film [7].

In a theoretical model, it was proposed that dry friction dominates under the front part of the ski while a friction-induced meltwater film forms further along the ski base [2]. Colbeck [8] predicted a thickness of 0.43 μm as an upper limit for the thickness of this meltwater film at a skiing speed of 10 m/s.

Further modelling based on rotating tribometer experiments at 5 m/s suggested meltwater thicknesses of < 0.1 μm at −15 °C, 0.2 μm at −5 °C, and 1.2 μm near the melting point [9]. On ice, a frictional meltwater film thickness of approximately 0.3 μm was estimated [10].

To date, however, no experimental data exist to verify these predictions. Moreover, there is currently no theory that adequately describes or quantifies the transition from dry friction—observed under low pressure and low speed conditions [6]—to the lubricated friction due to meltwater film formation that is expected under realistic skiing conditions [8].

The presumed frictional meltwater film is not stable after a ski passes over the snow. At sub-zero snow temperatures, any meltwater generated by friction begins to refreeze almost immediately. At 0 °C, the snow is typically so wet that any additional frictional meltwater is difficult to distinguish, making direct detection particularly challenging. In addition to the aforementioned attempts at direct detection, indirect methods have also been employed. For instance, the morphology of snow grains in photographs has been analyzed to infer melting and refreezing processes [8, 11]. However, to the best of our knowledge, no study has yet directly observed the refreezing of frictional meltwater. The objective of the present study was to verify the presence of meltwater by identifying signs of its refreezing under realistic skiing conditions, through the analysis of snow surface temperatures.

[1] Department of Sport Science, University of Innsbruck, Innsbruck 6020, Austria. [2] Research Center Snow, Ski, and Alpine Sport, Innsbruck 6020, Austria.

✉ Corresponding author. E-mail: Michael.hasler@fssa.at

Received: May 15, 2025; Revised: September 3, 2025; Accepted: September 11, 2025

2 Method

2.1 Friction testing

The experimental setup has been described in detail in a previous publication [12]. For clarity and ease of understanding, the key features are summarized here.

The experiments were conducted using a linear snow tribometer located in the snow laboratory of the Research Center for Snow, Ski, and Alpine Sport at the University of Innsbruck, Austria [13]. The test samples included a cross-country ski (Fischer RCS Skating Cold, 186 cm, Fischer Sports GmbH, Austria) and a flat-sliding sample without camber, with dimensions as shown in Fig. 1. The leading and trailing edges were rounded with a radius of 0.2 m. The sample was made of a core of medium-density fiberboard (MDF) with a sheet of a ski racing base (ultra-high molecular weight polyethylene (UHMWPE)), which was ground with the same parameters as the XC ski. The flat ski was mounted below an aluminum profile. We measured the pressure distribution of the flat sample with 4 kPa at the centre, decreasing to 1.4 kPa at the tip and tail by measuring the deformation of an elastomer under the ski [14]. With the same method, a pressure range of 0–40 kPa was found for the XC ski. After grinding, a liquid wax (Hydro warm, HWK-Kronbichler GmbH, Austria) was applied to XC ski and sample.

The sample was first accelerated and then moved over the snow surface at a constant speed, during which the friction force was measured. After each run, the slider was lifted off the snow and returned to the starting position. This took 15 s. Then, the sample was placed on the snow track again, and we waited a further 10 s. In preliminary tests, the temperature of the ski base was measured at this time. It remained stable at the snow temperature for all runs and speeds.

After each run, the sample was returned to the starting position. Each measurement series consisted of five repeated runs and was conducted on freshly prepared snow. An overview of the test conditions is provided in Table 1. The error of the friction measurements is speed dependent and changes from below 1% at 10 m/s, reaching up to 8% at 25 m/s.

The load conditions applied to the XC ski and the flat sample are not directly comparable. For the cross-country ski, the normal force was selected to represent realistic conditions—approximately half the weight of an athlete. Applying a similar pressure to the flat sample, however, would have resulted in the formation of deep tracks in the snow due to the destruction of the snow matrix. In such a case, the contact spots of the snow would continuously change, and the surface temperatures would not be comparable to the XC ski. Therefore, a lower normal force was applied to the flat sample to maintain similar friction mechanisms and ensure accurate thermal measurements.

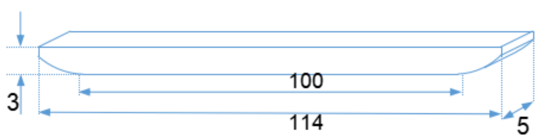

Fig. 1 Dimensions (in cm) of the sample [12].

2.2 Infrared measurements

An infrared camera (TE-EQ1, Thermal Experts, Republic of Korea) was mounted above the gliding track in the constant-speed section of the friction measurement. Each measurement was recorded at a resolution of 384 × 288 at a frame rate of $f = 30$ Hz. A surface area of 15 mm in width and 0.15 m in length along the sliding path of the ski or sample was selected for analysis. For each pixel within this area, the average temperature $\overline{\boldsymbol{T}_{i,j}}$ was calculated over a 10 s period following the passage of the ski or sample (defined as time t_0).

$$\overline{\boldsymbol{T}_{i,j}} = \frac{1}{10f}\sum_{t_0}^{t_0+10} T_{i,j}(t) \tag{1}$$

This calculation delivered an average temperature matrix $\overline{\boldsymbol{T}_{i,j}}$. Then, we determined the positions of the 10 highest temperatures in this matrix and retrieved the time course of these 10 pixels. For each frame, we subsequently calculated the average of the 10 temperatures, obtaining $T_{\text{hot10}}(t)$.

2.2.1 *Temperature reference*

The general error of the infrared measurements is specified to be below 2 K or 2%, accounting for uncertainties related to emissivity, reflected ambient temperature, transmittance, atmosphere temperature, camera response, or calibrator temperature accuracy. The detector sensitivity is 50 mK. To reduce the relatively high uncertainty, for reference, the temperature of the snow surface at a position which is also visible in the infrared pictures was simultaneously measured by a sensor (PT1000, Nexensos W-EYK, Heraeus Holding GmbH, Germany) and an 18 Bit data logger (Datataker DT80, ThermoFisher Scientific, USA). The difference between the precisely measured reference temperature and the corresponding pixel in the infrared image was subtracted from all image pixels to correct for systematic infrared measurement errors.

2.3 Heat dissipation mechanisms

The temperature of an object changes due to thermal convection, conduction, radiation, and additional exothermic or endothermic processes. The following sections aim to estimate the magnitude of each of these mechanisms and to describe their evolution over time.

Using Stefan Boltzmann's law, the radiative energy loss of a body at temperature T_1 in an environment at temperature T_2 can be calculated.

$$\frac{\dot{Q}}{A} = \varepsilon\sigma\left(T_1^4 - T_2^4\right) \tag{2}$$

Table 1 Test samples and testing speeds and temperatures

Sample	Cross-country ski	Flat sliding sample sample
Roughness, R_a (μm)	7	8
Normal force (N)	428	126
Average normal pressure (kPa)	5	2.4
Normal pressure range (kPa)	0–40	1.4–4
Temperature (°C)	−4	−4
Speed (m/s)	5, 10, 15, and 25	5, 10, 15, and 25

Assuming an emissivity ε of 0.9 [15] and the Stefan-Boltzmann constant σ, the specific radiative power at a temperature difference of 4 °C is approximately 16 W/m^2.

Thermal convection power (heat flux $\dot{Q}$ over area A) can be calculated using Eq. (3):

$$\frac{\dot{Q}}{A} = \alpha (T_1 - T_2) \tag{3}$$

where α is the heat transfer coefficient, T_1 is the temperature of the snow surface, and T_2 is the air temperature. Assuming a relatively low heat transfer coefficient of α = 3 W/(m^2·K) [16], a snow surface temperature T_1 of 0 °C at the contact spots, and an air temperature T_2 of −4 °C, the resulting specific convective heat loss is 12 W/m^2.

Thermal conduction can be approximated using Fourier's law:

$$\frac{\dot{Q}}{A} = \lambda \frac{T_1 - T_2}{d} \tag{4}$$

where λ is the thermal conductivity, T_1 and T_2 are the temperatures at a contact spot and at a vertical distance d from the contact spot, respectively. Immediately after the sample has passed, the snow surrounding the contact spots is assumed to be still at bulk temperature. Finite elements calculations [9] suggest that the snow temperature directly behind a slider is at the bulk temperature at more than 0.5 mm below the snow surface. Assuming a relatively large distance of d = 1 mm and a low snow thermal conductivity of λ = 0.1 W·m^{-1}·K^{-1} [17], the resulting specific conductive heat flux is approximately 400 W/m^2. This estimate likely underrepresents the actual maximum conductive power.

The calculated thermal conduction power is more than one order of magnitude higher than that of thermal convection and radiative heat loss. The temperature decay due to convective and conductive cooling is typically exponential because both mechanisms follow first-order differential equations in time, which naturally lead to exponential behavior.

When skiing over a patch of snow, a finite amount of energy is applied to the snow surface over a short time, and this energy subsequently dissipates into the snowpack. The transient heat conduction in such a scenario has been analytically described [18]. According to their solution, the temperature distribution in a semi-infinite homogeneous solid following an instantaneous heat pulse at the surface ($x = 0, t = 0$) is given by

$$T(t, x) = T_{\text{env}} + (T_0 - T_{\text{env}}) t^{-\frac{1}{2}} \mathrm{e}^{-\frac{x^2}{4\kappa t}} \tag{5}$$

This equation describes the temperature $T(t, x)$ as a function of time t and depth x, with T_0 being the initial surface temperature, T_{env} the ambient (bulk snow) temperature, and κ the thermal diffusivity of snow.

If frictional meltwater was present, its latent heat of fusion must also be considered. The change of enthalpy of water is 333.55 J/kg during the freezing process. In theory, this latent heat maintains the water at 0 °C until complete solidification occurs.

A recent review on snow and ice friction mechanisms also considered the quasi-liquid layer (QLL), a thin film of water that forms on the surface of ice crystals [19]. While several studies have investigated the role of the QLL in friction on compact ice surfaces (e.g., Refs. [20–22]), its significance in ski–snow friction remains uncertain. A brief estimation of the QLL's potential contribution to surface temperature change may be helpful. Assuming a QLL thickness of 30 nm [23] and an exceptionally high contact area of 50% [2], the resulting mass of the QLL is approximately 1.5×10^{-2} g per square meter. Considering the enthalpy of fusion for water and a heat input of 400 W from above, the corresponding time scale is roughly 10 ms. Therefore, the QLL does not significantly influence the long-term temperature development examined in this work.

To analyze the temperature data following the passage of the ski or sample, the cooling curve is segmented into distinct phases. An exponential temperature decrease indicates that convective and conductive heat transfer, as described by Fourier's law, dominate the cooling process. In contrast, any deviation from exponential behavior may suggest the presence of re-freezing meltwater.

For this analysis, infrared images recorded over a 10-s interval after the sample passage—corresponding to 300 frames—are evaluated.

We hypothesize that the 10-s interval consists of two phases:

(1) Phase I: An initial period influenced by meltwater re-freezing, characterized by non-exponential behavior.

(2) Phase II: A subsequent phase governed by exponential cooling.

The temperature profile during Phase I is best approximated by a linear fit, while Phase II follows an exponential decay. The exponential portion is modeled using the function:

$$f(t) = A + B\mathrm{e}^{-\alpha t} \tag{6}$$

where A and B are free parameters. To identify the transition point between these phases, the index i is determined such that the combination of a linear fit from frame P_0 to P_i and an exponential fit from P_{i+1} to P_{300} provides the best approximation of the measured temperature data. This is achieved using a least-squares minimization approach. The resulting value of i indicates the time at which the system transitions from a re-freezing-dominated regime to a cooling process consistent with Fourier's law (Fig. 2, at t = 1.9 s).

3 Results

3.1 Friction

The coefficient of friction increases with increasing speed. While below 15 m/s, the coefficient of friction of the XC ski is slightly lower than that of the sliding sample, at 25 m/s it is clearly higher (Fig. 3). It should be noted that although the coefficients of friction are similar, the power of friction differs by approximately a factor of three due to the different normal force.

3.2 Heat dissipation mechanisms

The onset time of the exponential decay phase (1.9 s in Fig. 2) was found to depend on both the sliding speed and the number of

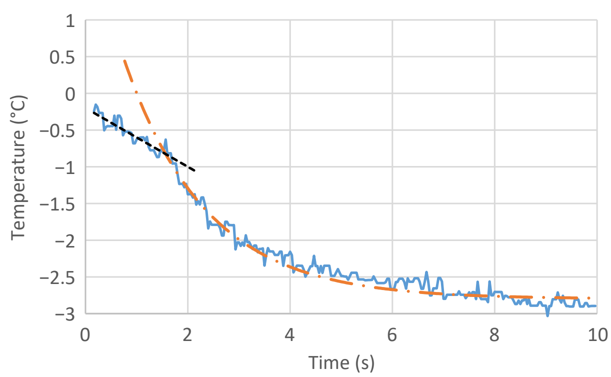

Fig. 2 Snow temperature T_{hot10} (blue, full line) vs. time after passage with linear (dots, black) and exponential fit (dash-dot, orange).

清華大学出版社 Tsinghua University Press | SciOpen

runs on the same track. A distinct non-exponential phase—indicative of meltwater re-freezing—was observed only in the case of the XC ski at velocities of 15 and 25 m/s. At 25 m/s, a non-exponential phase lasting 0.5 s was first detected after the third run, increasing to 1.9 s by the fifth run. At 15 m/s, a non-exponential phase of 0.5 s appeared only after the fifth run. In contrast, the temperature profile behind the flat sliding sample without camber exhibited purely exponential behavior in all cases, with no indication of a preceding non-exponential phase.

4 Discussion

4.1 Heat dissipation mechanisms

The snow temperature decreased after the passage of the ski/sample. The decrease revealed two distinct cooling phases (Fig. 2). At high speeds and after multiple runs with the XC ski, the initial temperature decrease followed an approximately linear trend before transitioning to an exponential decay. This transition phase lasted up to 2 s.

Initially, frictional meltwater refreezes at a theoretically constant temperature. However, since each pixel in the infrared image covers an area of approximately 1 mm^2—larger than individual contact spots—the observed signal represents a superposition of regions with meltwater refreezing at 0 °C and others undergoing conductive/convective cooling. Once refreezing is complete, the resulting solid (snow and frozen meltwater) cools according to Fourier's law.

This two-phase behavior was only observed after repeated runs on the same surface. Micro-computed tomography studies in similar snow conditions on the same snow type showed that the relative contact area rises from 9% after one run to 27% after 10 runs [24]. Although a larger contact area should theoretically distribute frictional heat over a wider surface, thereby reducing temperature, the opposite was observed—surface temperatures rose. This suggests another mechanism is responsible for the onset of meltwater generation after multiple runs. One hypothesis involves the temperature of the ski base. Although the surface temperature of the ski was not directly measured, a consistent 10 s break between runs ensured that both ski and snow maintained stable thermal contact and likely consistent temperature.

An alternative explanation lies in the evolving snow-ski interface. As the contact area increases, so does the sheared cross-section. The shear force is given by $F_S = \tau_{ice} A_c$ with τ_{ice} the shear strength of ice and A_c the contact area. Once this sheared cross-section becomes large enough, the snow grains may no longer break as easily. Consequently, the friction mechanism might shift from abrasion [19] to frictional meltwater lubrication. Such a transition was not observed with the flat sliding sample. One likely reason is the significantly lower frictional power, which was approximately three times lower than in the XC ski experiments—possibly insufficient to generate detectable meltwater. Due to the different pressure distributions below the flat sample and XC ski (maximum pressure 4 kPa vs. 40 kPa [25], the difference in area-specific power was even more pronounced. At 25 m/s, frictional meltwater was detected behind the XC ski but not behind the flat test specimen. At this speed, the maximum area-specific power below the flat sample reached only 10 kW/m^2, whereas the pressure peaks on the XC ski produced 135 kW/m^2. It is to be expected that this maximum local power is essential for the formation of friction meltwater.

The geometry of the ski tip relative to the flat sample tip may also contribute to the observed differences. For the flat sample, the pressure gradient at the tip can be approximated. The pressure near the tip was measured at 1.4 kPa. Based on measurements of the viscoelastic properties of snow [26], the deformation of a pre-compacted artificial snow cover under this load is estimated to be approximately 3 μm. With a tip radius of 0.2 m, this corresponds to a contact length of roughly 1 mm. At a velocity of 5 m/s, the resulting rate of pressure increase is approximately 6 MPa/s. In contrast, the pressure gradient at the ski tip is expected to be substantially lower due to the progressive reduction in curvature and the lower structural stiffness of the ski.

The thermal conductivity of pure UHMWPE is reported in the range of 0.4–0.5 W/(m·K), with a specific heat capacity of approximately 1,840 J/(kg·K) and a density of 0.93 g/cm^3 [27]. In practice, the thermal conductivity of ski base materials is expected to exceed that of pure UHMWPE due to the incorporation of additives such as carbon, although quantitative data are not available. On the snow side, our compacted snow with a density of 400 kg/m^3 exhibits a thermal conductivity of approximately 0.3 W/(m·K) and a specific heat capacity of ~850 J/(kg·K) [28]. A simple estimation indicates that, when the ski base thermal conductivity increases from 0.4 to 0.8 W/(m·K) at a frictional power density of 2,000 W/m^2, the fraction of heat dissipated into the ski increases from 72% to 79%. This corresponds to a reduction of approximately 25% in the power available for heat transfer into the snow.

4.2 Friction

In general, the friction of cross-country (XC) skis increases with speed at higher temperatures [29]. The variation of the coefficient of friction with speed in this experiment has already been discussed in a previous paper [12]. Here, we focus on a specific observation: While both the flat sample and XC ski exhibit similar coefficients of friction at 5, 10, and 15 m/s, a significant divergence appears at 25 m/s, where the XC ski shows substantially higher friction. This difference can be attributed primarily to two factors. First, the pressure distribution differs between the two samples: the flat sample exhibits a flat pressure distribution with pressures between 1.4 and 4 kPa, whereas the XC ski has zones without snow contact and two pronounced pressure peaks up to 40 kPa [25]. Due to a lower applied normal force, the flat sliding sample generates less frictional power.

The higher peak pressure beneath the XC ski may cause greater deformation of the snow and increased surface wear. However, this effect is expected to be relatively independent of speed. In contrast, the greater frictional power of the XC ski results in significantly higher surface temperatures [12]. Yet, since the temperature difference between the XC ski and the flat sample remained roughly constant across all speeds, snow temperature

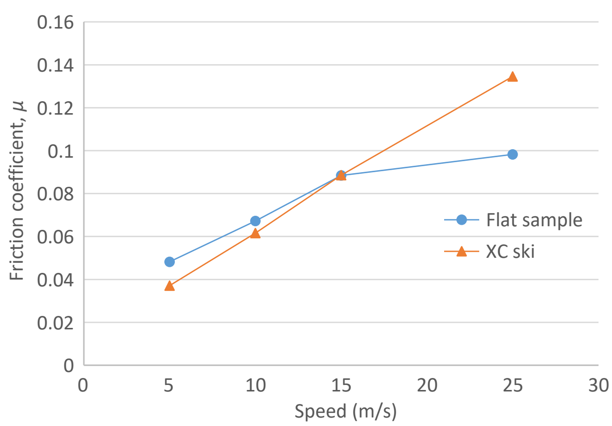

Fig. 3 Coefficient of friction μ vs. speed for the flat sliding sample (blue circles) and the XC ski (orange triangles).

alone cannot account for the different friction behaviors observed at high speed. What is particularly striking is that, especially at 25 m/s—where multiple indicators of frictional meltwater were observed—the flat sliding sample, which showed no detectable meltwater, exhibited lower friction. This supports the conclusion, consistent with several other studies [8, 29, 30], that excessive frictional meltwater can lead to increased friction.

4.3 Water film

We identified several indicators suggesting the presence of a water film beneath the XC ski. The most compelling evidence—manifested as two distinct heat dissipation mechanisms—was observed at high speeds and after multiple passes over the same snow surface. However, this does not rule out the presence of meltwater under less extreme conditions. Rather, the limitations of the current setup—namely, the lack of precise knowledge of the actual contact area and the restricted spatial and thermal resolution of the infrared camera—reduce its sensitivity in detecting thinner or more transient water films. Importantly, our measurements only capture the state of the snow surface after the passage of the ski or sample. It remains plausible that a thin water film forms beneath the ski during sliding but refreezes too rapidly to be detected afterwards.

5 Conclusions

Using infrared imaging on a large-scale linear snow tribometer, we identified indicators of meltwater formation during sliding friction under realistic skiing conditions. Temperature profiles revealed signatures consistent with a freezing process occurring under specific circumstances. Notably, the results varied significantly between a real cross-country (XC) ski and a flat sample ski without camber. This discrepancy is likely due to differences in pressure distribution and contact mechanics, leading to variations in the thickness and behavior of the frictional meltwater film.

Acknowledgements

The authors acknowledge support from the Austrian Science Fund (FWF): [P36489-N].

Declaration of competing interest

The authors have no competing interests to declare that are relevant to the content of this article.

Ethical approval

This study does not contain any studies with human or animal subjects performed by any of the authors.

References

[1] Bowden F P, Hughes T P. The mechanism of sliding onf ice and snow. *Proc R Soc Lond Ser-A* **172**(949): 280–298 (1939)

[2] Colbeck, S. C. A review of the processes that control snow friction. Monograph 92-2, US Army Cold Regions Research and Engineering Laboratory, Hanover, NH, USA, 1992.

[3] Ambach W, Mayr B. Ski gliding and water film. *Cold Reg Sci Technol* **5**(1): 59–65 (1981)

[4] Colbeck S C. The kinetic friction of snow. *J Glaciol* **34**: 78–86 (1988)

[5] Strausky H, Krenn J R, Leitner A, Aussenegg F R. Sliding plastics on ice: Fluorescence spectroscopic studies on interfacial water layers in the µm thickness regime. *Appl Phys B-Lasers O* **66**(5): 599–602 (1998)

[6] Lever J H, Taylor S, Song A J, Courville Z R, Lieblappen R, Weale J C. The mechanics of snow friction as revealed by micro-scale interface observations. *J Glaciol* **64**(243): 27–36 (2018)

[7] Lever J H, Taylor S, Hoch G R, Daghlian C. Evidence that abrasion can govern snow kinetic friction. *J Glaciol* **65**(249): 68–84 (2019)

[8] Colbeck S C. A review of the friction of snow skis. *J Sports Sci* **12**(3): 285–295 (1994)

[9] Bäurle L, Kaempfer T U, Szabó D, Spencer N D. Sliding friction of polyethylene on snow and ice: Contact area and modeling. *Cold Reg Sci Technol* **47**(3): 276–289 (2007)

[10] Evans D C B, Nye J F, Cheeseman K J. The kinetic friction of ice. *P Roy Soc Lond A Mat* **347**(1651): 493–512 (1976)

[11] Huzioka T, Kinosita S. Studies on the resistance of a snow sledge III. Friction between snow and a plastic plate. *Low Temp Sci A* **20**: 159–180 (1962)

[12] Hasler M, Jud W, Nachbauer W. Snow temperature behind sliding skis as an indicator for frictional meltwater. *Front Mech Eng* **7**: 738266 (2021)

[13] Hasler M, Schindelwig K, Mayr B, Knoflach C, Rohm S, van Putten J, Nachbauer W. A novel ski–snow tribometer and its precision. *Tribol Lett* **63**(3): 33 (2016)

[14] M. Mössner, K. Schindelwig, D. Heinrich, M. Hasler, W. Nachbauer. Effect of load, ski and snow properties on apparent contact area and pressure distribution in straight gliding. *Cold Reg Sci Technol* **208**: 103799 (2023)

[15] Hori M, Aoki T, Tanikawa T, Motoyoshi H, Hachikubo A, Sugiura K, Yasunari T J, Eide H, Storvold R, Nakajima Y, et al. *In-situ* measured spectral directional emissivity of snow and ice in the 8–14 µm atmospheric window. *Remote Sens Environ* **100**(4): 486–502 (2006)

[16] Mills A F. *Heat Transfer*. Florida (USA): CRC Press, 1992.

[17] Sturm M, Holmgren J, König M, Morris K. The thermal conductivity of seasonal snow. *J Glaciol* **43**(143): 26–41 (1997)

[18] Carslaw H S, Jaeger J C. Conduction of heat in solids. In: *SFPE Handbook of Fire Protection Engineering Springer*. Hurley M J, Gottuk D, Hall J R, et al. Eds. New York: Springer, 1959: 25–52.

[19] Lever J H, Asenath-Smith E, Taylor S, Lines A P. Assessing the mechanisms thought to govern ice and snow friction and their interplay with substrate brittle behavior. *Front Mech Eng* **7**: 690425 (2021)

[20] Weber B, Nagata Y, Ketzetzi S, Tang F J, Smit W J, Bakker H J, Backus E H G, Bonn M, Bonn D. Molecular insight into the slipperiness of ice. *J Phys Chem Lett* **9**(11): 2838–2842 (2018)

[21] Nagata Y, Hama T, Backus E H G, Mezger M, Bonn D, Bonn M, Sazaki G. The surface of ice under equilibrium and nonequilibrium conditions. *Accounts Chem Res* **52**(4): 1006–1015 (2019)

[22] Louden P B, Gezelter J D. Why is ice slippery? simulations of shear viscosity of the quasi-liquid layer on ice. *J Phys Chem Lett* **9**(13): 3686–3691 (2018)

[23] Döppenschmidt A, Butt H J. Measuring the thickness of the liquid-like layer on ice surfaces with atomic force microscopy. *Langmuir* **16**(16): 6709–6714 (2000)

[24] Hasler M, Mössner M, Jud W, Schindelwig K, Gufler M, van Putten J, Rohm S, Nachbauer W. Wear of snow due to sliding friction. *Wear* **510–511**: 204499 (2022)

[25] Schindelwig K, Hasler M, Van Putten J, Rohm S, Nachbauer W. Temperature below a gliding cross country ski. *Procedia Engineer* **72**: 380–385 (2014)

[26] Theile T, Szabo D, Luthi A, Rhyner H, Schneebeli M. Mechanics of the ski–snow contact. *Tribol Lett* **36**(3): 223–231 (2009)

[27] Information on https://analyzing-testing.netzsch.com/en/polymers-netzsch-com/commodity-thermoplastics/pe-uhmw-polyethylene-ultra-high-molecular-weight.

[28] Information on https://usace.contentdm.oclc.org/digital/collection/p266001coll1/id/7366.

[29] Yen Y C. Review of thermal properties of snow, ice, and sea ice, U.S. Army Cold Regions Research and Engineering Laboratory (CRREL). Hanover, NH, USA, 1981

[30] Bowden F P. Friction on snow and ice. *Proc R Soc Lond Ser-A* **217**(1131): 462–478 (1953)

Michael Hasler is an Austrian researcher specializing in friction on snow and ice, sports engineering, and biomechanics, with a particular focus on alpine sports. He serves as senior researcher at the Research Center Snow, Ski, and Alpine Sport, Innsbruck, Austria. His academic background includes studies in experimental physics at the University of Innsbruck, Innsbruck, Austria, a B.Sc. degree in environmental, process and control engineering at Management Center Innsbruck, Innsbruck, Austria, an M.Sc. degree in industrial engineering and management at Management Center Innsbruck, Innsbruck, Austria, and a Ph.D. degree in biomechanics at the University of Innsbruck, Innsbruck, Austria. His main research areas encompass measurement engineering, friction on snow and ice, sports engineering, and biomechanics in alpine sports. With his interdisciplinary expertise in physics, engineering, and biomechanics, Dr. Hasler makes significant contributions to enhancing performance and safety in snow and alpine sports disciplines.